Biomedicine & Pharmacotherapy 130 (2020) 110515

Contents lists available at ScienceDirect

Biomedicine & Pharmacotherapy

journal homepage: www.elsevier.com/locate/biopha

Original article

Chloroacridine derivatives as potential anticancer agents which may act as tricarboxylic acid cycle enzyme inhibitors

Miroslawa Cichorek[a,*], Anna Ronowska[b], Krystyna Dzierzbicka[c], Monika Gensicka-Kowalewska[c], Milena Deptula[a], Iwona Pelikant-Malecka[d,e]

[a] Department of Embryology, Medical University of Gdansk, Debinki 1 St. PL, 80-210, Gdansk, Poland
[b] Department of Laboratory Medicine, Medical University of Gdansk, Debinki 7 St. PL, 80-211, Gdansk, Poland
[c] Department of Organic Chemistry, Gdansk University of Technology, Narutowicza St. 11/12. PL, 80-233, Gdansk, Poland
[d] Department of Biochemistry, Medical University of Gdansk, Debinki 1 St. PL, 80-210, Gdansk, Poland
[e] Department of Medical Laboratory Diagnostics, Central Bank of Frozen Tissues and Genetic Specimens, Medical University of Gdansk, Biobanking and Biomolecular Resources Research Infrastructure Poland, Debinki 7 St. PL, 80-211, Gdansk, Poland

ARTICLE INFO

Keywords:
Chloroacridine
Amelanotic melanoma
Melanotic melanoma
Apoptosis
Tricarboxylic acid cycle enzymes
Cell death

ABSTRACT

Purpose: This paper concerns the cytotoxicity of 9-chloro-1-nitroacridine (**1a**) and 9-chloro-4-methyl-1-nitroacridine (**1b**) against two biologically different melanoma forms: melanotic and amelanotic. Melanomas are tumors characterized by high heterogeneity and poor susceptibility to chemotherapies. Among new analogs synthesized by us, compound **1b** exhibited the highest anticancer potency. Because of that, in this study, we analyzed the mechanism of action for 1a and its 4-methylated derivative, **1b**, against a pair of biological melanoma forms, with regard to proliferation, cell death mechanism and energetic state.

Methods: Cytotoxicity was evaluated by XTT assay. Cell death was estimated by plasma membrane structure changes (phosphatidylserine externalization), caspase activation, and ROS presence. The energetic state of cells was estimated based on NAD and ATP levels, and the activity of tricarboxylic acid cycle enzymes (pyruvate dehydrogenase complex, aconitase, isocitrate dehydrogenase).

Results: The chloroacridines affect biological forms of melanoma in different ways. Amelanotic (Ab) melanoma (with inhibited melanogenesis and higher malignancy) was particularly sensitive to the action of the chloroacridines. The Ab melanoma cells died through apoptosis and through death without caspase activation. Diminished activity of TAC enzymes was noticed among Ab melanoma cells together with ATP/NAD depletion, especially in the case of **1b**.

Conclusion: Our data show that the biological forms of the tumors responded to **1a** and its 4-methylated analog in different ways. **1a** and **1b** could be inducers of regulated melanoma cell death, especially the amelanotic form. Although the mechanism of the cell death is not fully understood, **1b** may act by interfering with the TAC enzymes and blocking specific pathways leading to tumor growth. This could encourage further investigation of its anticancer activity, especially against the amelanotic form of melanoma.

1. Introduction

In the search for a cure for melanoma, new methods of early diagnosis, surgical excision and new adjuvant therapies have produced more positive responses than in earlier years [1–4]. Unfortunately, a large number of melanoma patients develop drug resistance during their treatment [5–8]. Therefore, new compounds that would enhance the effects of melanoma treatment are highly desirable. Melanomas are molecularly heterogeneous neoplasm. Melanoma has been classified into subtypes based on the tissue from which the primary tumor arises (skin, eye, mucous membranes) and histological analysis (superficial spreading, lentigo maligna, nodular, acral lentiginous, desmoplastic, amelanotic) [7,9,10]. Despite significant progress in the understanding of the molecular alterations in melanomas, the degree of melanoma molecular heterogeneity that is associated with its histologic heterogeneity is still unknown [10–12]. The striking features of melanoma as high genetic instability, cell plasticity in response to perceived changes in the microenvironment, dedifferentiation to a variety of states under cellular stress, drives therapy resistance [13–16]. Melanoma is a highly aggressive solid tumor, showing also an impressive metabolic plasticity

* Corresponding author.
E-mail address: miroslawa.cichorek@gumed.edu.pl (M. Cichorek).

https://doi.org/10.1016/j.biopha.2020.110515
Received 13 March 2020; Received in revised form 3 July 2020; Accepted 7 July 2020

modulated by oncogenic activation [17,18]. The possible switch between diverse phenotypic states creates a plethora of opportunities for melanoma cells to escape the treatment [19–21]. Heterogeneity and plasticity of melanoma cells are well recognized as causative factors of chemoresistance [8,15,16,19,22,23].

Based on cell's ability to synthesize melanin, melanomas can also be divided into two biologically distinct forms: melanotic and amelanotic/hypomelanotic [24–26]. Amelanotic melanoma is very rare, making up 2–4 % of all melanomas [24,27], though some analyses report this figure to be as high as 20 % [26]. Cells of this melanoma type lack or show a decreased level of the melanogenesis process, and as a consequence the melanoma becomes nearly white in color [24,26,28]. According to the presence (melanotic melanoma) or absence (amelanotic melanoma) of melanogenesis, cell sensitivity to cure method may differ, however the level of melanoma cell pigmentation and the best method of treatment still remains a controversial subject [28–32].

Acridines are heteroaromatic compounds with a wide range of biological activities as anticancer, anti-inflammatory, antimicrobial, antiparasitic, antiviral and fungicidal agents [33,34]. Acridines are capable to bind nucleic acids by hydrophobic interactions namely intercalation, i.e. auto-insertion between two adjacent base pairs of nucleic acids that influence many cell processes [35–37]. However, the more recent studies favor an explanation based on direct interaction of acridines with biologically important proteins [33,38,39]. Thus in reference to these properties, acridines are explored as potential anticancer compounds [38,33,39].

Our previous studies indicated that the Ab amelanotic melanoma of the Bomirski hamster melanoma model is particularly sensitive to a new acridine-retro-tuftsin compound, when compared to the melanotic Ma line of the same model [40,41]. Having considered that, in this paper we present antimelanoma research with 9-chloroacridine and its methylated derivative 9-chloro-4-methyl-1-nitroacridine (Fig.1), the preparation of which is one of the steps for the synthesis of acridines by the Ullmann condensation method. According to our knowledge, the anticancer activity of these compounds has not been studied before although the 9-chloroacridines are the common precursors for obtaining new acridine derivatives at position 9 [33].

The most commonly used method of acridine synthesis is the cyclization of *N*-phenylanthranilic acid derivatives obtained as a result of Ullmann condensation. This reaction generates by-products (probably products of chlorination of other acridine core positions), which were separated by TLC. The 9-chloroacridine derivatives were further isolated and purified by usual techniques [42–48].

Among new analogs synthesized by us, the compound 9-chloro-4-methyl-1-nitroacridine (**1b,** Fig.1) exhibited the highest anticancer potency. C4-methyl substituents significantly affect thermodynamic mechanisms associated with complex formation and molecular interactions between the ligand and its DNA binding site and as such could influence the biological activity [49]. In this study, we analyzed the mechanism of action of 9-chloro-1-nitroacridine and its 4-methylated derivative against a pair of biological forms of melanoma (melanotic, amelanotic), in terms of proliferation, cell death mechanism, and energetic state.

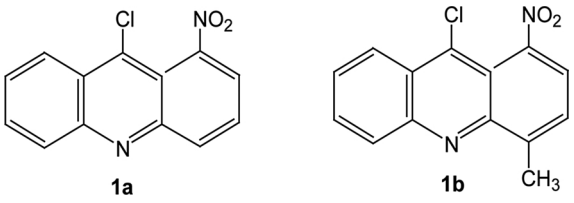

Fig. 1. Structure of 9-chloro-1-nitroacridine **1a** and 9-chloro-4-methyl-1-nitroacridine **1b.**

2. Material and methods

2.1. Transplantable melanomas – Bomirski hamster melanoma model

The original transplantable melanotic melanoma (Ma) was derived from a spontaneous melanoma of the skin that had appeared in a breed of golden hamster [50]. The amelanotic melanoma line (Ab) originated from the Ma form by a spontaneous alteration. The loss of melanin was accompanied by changes in many biological features of the Ab line – faster tumor growth rate, shorter animal survival, and changes in cell ultrastructure [50,51]. Since their discovery, each melanoma line has been maintained in vivo by consecutive, subcutaneous transplantations of tumor material every 21 (Ma) or 11 (Ab) days. The hamsters were injected with a suspension of melanoma tissue obtained by mincing in a glass homogenizer. The tumor tissue was injected subcutaneously into the flank region in an amount of 200 mg of Ma per one hamster and 50 mg of Ab melanoma per one hamster. Differences in the quantity of transplanted tumors and time of getting animals for experiments were adequate to the known rate of growth of these two melanoma lines [50].

Pathobiological characteristic of Bomirski hamster melanoma model is described in the Supplementary material (S1. Pathobiological BHM model characteristic).

All experiments were conducted in accordance with a Guide for the Care and Use of Laboratory Animals published by the European Parliament, Directive 2010/63/EU and were performed with approval of the Animal Ethics Committee at the Medical University of Gdansk (24/2015).

2.2. Isolation of melanotic and amelanotic melanoma cells

Melanoma cells were isolated for each experiment from solid tumors by a non-enzymatic, mechanical dissociation of tissue (taken at the time of routine passages). The melanoma cells were isolated by means of a density gradient of Histopaque-1077 (Sigma-Aldrich, USA) [52]. The suspension consisted of 95–98 % viable cells (estimated by trypan blue test).

2.3. Synthesis of acridine compounds 9-chloro-1-nitroacridine (1a) and 9-chloro-4-methyl-1-nitroacridine (1b) (Fig. 1)

The preparation of 9-chloro-1-nitroacridine was done by an Ullmann condensation reaction of the potassium salt of *o*-chlorobenzoic acid **2** and *m*-nitroaniline **3a** in the presence of copper at 125 °C to give *N*-(3′-nitrophenyl)anthranilic acid **4a**, which was refluxed in $POCl_3$ to afford the 9-chloroacridine derivative **1a** [45–47,53,54]. 9-Chloro-4-methyl-1-nitroacridine **1b** was synthesized in two steps: Ullmann reaction of *o*-chlorobenzoic acid with 3-nitro-6-methylaniline in the presence of anhydrous potassium carbonate and copper(II), cyclization of *N*-(2′-methyl-5′-nitrophenyl)anthranilic acid **4b** to derivative **1b** (Fig. 2) [41]. The final products **1a**,**b** was purified with preparative TLC and its identity was confirmed by high resolution ^{1}H NMR (500 MHz), ^{13}C NMR (125 MHz) and MS mass spectrometry analysis (MALDI-TOF MS, Biflex III Bruker).

The general preparation of 1-nitro-9-chloroacridine (**1a**) and 9-chloro-4-methyl-1-nitrocridine (**1b**) was described in literature [43,45,46,48].

o-Chlorobenzoic acid (127.7 mmol) was dissolved in 1 L of water and added in portions of KOH (about 139 mmol) to pH = 7. The water was evaporated. A mixture of potassium salt of *o*-chlorobenzoic acid (62.5 mmol), *m*-nitroaniline or 3-nitro-6-methylaniline (187.5 mmol) and freshly precipitated copper dust (1.2 mmola) was heated at 125 °C for 1 h. Then, the hot melt was poured into 0.3 ml of intensely stirring hot 5% potassium carbonate solution. The mixture was heated to reflux with the addition of activated carbon, and filtered. After cooling, the precipitated excess of *m*-nitroaniline or 3-nitro-6-methylaniline was

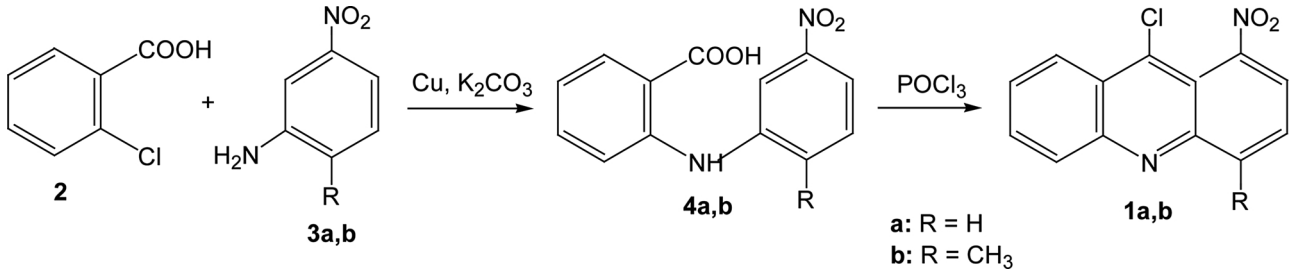

Fig. 2. Synthesis of 9-chloro-1-nitroacridine **1a** and 9-chloro-4-methyl-1-nitroacridine **1b.**

filtered off. The filtrate was acidified with conc. HCl up to pH = 5−6. The precipitate was filtered. The crude product was crystallized from ethanol, obtaining *N*-(3′-nitrophenyl)anthranilic acid or *N*-(2′-methyl-5′-nitrophenyl)anthranilic acid. Then, a mixture of *N*-(3′-nitrophenyl) anthranilic acid derivatives (26.6 mmol) and of $POCl_3$ (266 mmol) was heated at 120 °C. After 20 min the excess of $POCl_3$ was distilled off. To the residue was added a small amount of chloroform, then the solution was poured into a mixture of NH_3:CH_3Cl (1:3) cooled to −70 °C. The organic layer was separated and dried with anhydrous $MgSO_4$. After filtration and distillation of the solvent, pyridine was added and the precipitate was filtered off. Then, the filtrate was heated at 60 °C for 20 min. After cooling, a 9-chloro-1-nitroacridine precipitate was obtained, melting point 150−151 °C [54].

9-Chloro-1-nitroacridine ***1a,*** Yield 84 %, yellow product; ^{1}H NMR (500 MHz, DMSO-d_6) δ ppm: 6.82 (m, 1H, 7), 7.37 (m, 2H, 6, 3), 8.21 (m, 2H, 2, 5), 8.40 (m, 2H, 4, 8); ^{13}C NMR (500 MHz, CD_3OD) δ ppm: 148.94 (C-9), 148.15 (C-1), 146.37 (C-4a), 137.25 (C-5a), 134.51 (C-6), 132.97 (C-2), 129.98 (C-8), 129.87 (C-7), 129.44 (C-4), 125.11 (C-5), 124.94 (C-8a), 124.50 (C-3), 115.16 (C-1a). MS *m/z* calculated for $C_{13}H_7ClN_2O_2$ 258.66 found 260.31 $[M+H]^+$.

9-Chloro-4-methyl-1-nitroacridine ***1b,*** Yield 82 %, yellow product; ^{1}H NMR (500 MHz, DMSO-d_6) δ ppm: 2.52 (s, 3H, Ar−CH3), 6.82 (m, 1H, 7), 7.37 (m, 2H, 6, 3), 8.21 (m, 2H, 2, 5), 8.40 (m, 2H, 4, 8); ^{13}C NMR (500 MHz, CD_3OD) δ ppm: 148.94 (C-9), 148.15 (C-1), 146.37 (C-4a), 137.25 (C-5a), 134.51 (C-6), 132.97 (C-2), 129.98 (C-8), 129.87 (C-7), 129.44 (C-4), 125.11 (C-5), 124.94 (C-8a), 124.50 (C-3), 115.16 (C-1a). MS *m/z* calculated for $C_{14}H_9ClN_2O_2$ 272.68; found 272.43 $[M+H]^+$.

2.4. Cell viability assay (XTT)

Cell viability was determined by XTT assay (Roche Diagnostic, USA) which measures the cells' ability to reduce the tetrazolium salt XTT (2.3-bis-(2-methoxy-4-nitro-5-sulfophenyl)-2*H*-tetrazolium-5-carboxanilide) to a water-soluble formazan product. Cells were seeded at a density of 5 × 10^3 for Ab melanoma and 50 × 10^3 for Ma melanoma cells into 96-well plates with suitable cultivation media. After 24 h the media were exchanged and cells were stimulated with appropriate concentrations (0.1–150 μM) of the examined compounds for 48 and 72 h. The orange-colored formazan product was quantified at 450 nm in a microplate reader (Multiscan FC. Thermoscientific USA). Cell viability was normalized with respect to an untreated control (100 %) and the half maximal inhibitory concentration IC_{50} was estimated. The tested compounds were primary dissolved in 0.10 mM DMSO then diluted to the final concentration in a growth medium. The final concentration of DMSO in the culture did not exceeded 0.001 mM and did not influence cellular viability.

2.5. Cytofluorimetric analysis of apoptosis

Flow cytometry analysis was the method used for estimation of activated caspases, plasma membrane changes (phosphatidylserine externalization), reactive oxygen species (ROS) and cell cycle changes. Cells were seeded in 6-well plates at a concentration of 200 × 10^3/well for Ab melanoma and 500 × 10^3 for Ma melanoma, incubated with **1a** and **1b** at 100 μM for Ma cells and at 15 μM for Ab cells, for 48 and 72 h. For the analysis in the flow cytometer 1 × 10^6 cells were stained with antibodies conjugated with fluorochrome, or the cells were incubated with fluorogenic substrate. After incubation the cells were analyzed using a C6 flow cytometer (Becton Dickinson Immunocytometry Systems, USA). After gating out small-sized (e.g. noncellular debris) objects, 10,000 events were collected from each sample. Results were analyzed off-line using Cyflogic v.1.2.1 software.

2.6. Activated caspases

We used a FLICA test (fluorochrome-labeled inhibitors of caspases) to estimate cells containing activated caspases [55]. The rationale for this method is that fluorochrome-labeled inhibitors of caspases covalently react with the reactive enzymatic center of activated caspases. We used a FITC (fluorescein) labeled pan-inhibitor of caspases, VAD-FMK, which detects most active caspases in the cell. After 48 and 72 h incubation with the acridines the cells were collected and 1 × 10^6 cells from each experimental point were incubated with 5 μM FITC-VAD-FMK (CaspACETM FITC-VAD-FMK, Promega, USA) for 30 min at room temperature in the dark. The cells were analyzed using a flow cytometer.

2.7. Phosphatidylserine (PS) externalization assay

An early apoptotic change of the plasma membrane structure, PS externalization, was determined by Annexin V-FITC and propidium iodide (PI) staining (BD Pharmingen, USA) according to the manufacturer's instructions. The staining allows populations of cells to be determined and categorized as: viable An-PI-; early apoptotic An+PI- [have green fluorescence (PS externalization) but excluded PI (plasma membrane is not damaged)]; late apoptotic An+PI+ [have green fluorescence (PS externalization) and stained PI (plasma membrane is damaged)]; and final apoptosis/necrosis An-PI+ [absence of green fluorescence (lack of PS externalization) and stained PI (plasma membrane is damaged)]. Fluorescence intensity was measured by a flow cytometer.

2.8. Reactive oxygen species

DCFDA (2′.7′-dichlorofluorescin diacetate), a fluorogenic dye, measures reactive oxygen species (ROS) activity within a cell. After diffusion into a cell, DCFDA is deacetylated by cellular esterases to a non-fluorescent compound, which is later oxidized by ROS into 2′.7′-dichlorofluorescein (DCF). DCF is a highly fluorescent compound which can be detected by flow cytometry. DCFDA (Sigma-Aldrich, USA) was added to cells according to the manufacturer's protocol, and after 30 min incubation at 37 °C the fluorescence intensity was analyzed in a flow cytometer. As a positive control, cells were incubated with 3% H_20_2 (1:30).

2.9. Cell cycle analysis

Cell cycle distribution was determined by the flow cytometry method, based on the DNA content in cell nuclei, as described earlier [56]. 1×10^6 ethanol-fixed cells were resuspended in 1 ml of a staining solution containing 40 μg/ml propidium iodide (Sigma Chemicals, USA) and 100 μg/ml RNase A (Sigma Chemicals, USA) and incubated for 30 min at 37 °C. Results were analyzed by flow cytometry.

2.10. Activity of enzymes as a function of the energetic state of cells

PDHC (pyruvate dehydrogenase complex; EC1.2.4.1), aconitase (EC4.2.1.3), NADP-isocitrate dehydrogenase (ICDH; EC1.1.1.42), lactate dehydrogenase (LDH EC1.1.1.27) activities were estimated in cell lysates after 48 h culture with **1a** and **1b**. Cells were harvested into ice cold Puck's solution (140 mmol/L NaCl, 5 mmol/L KCl, 5 mmol/L glucose, 1.7 mmol/L Na-phosphate buffer, pH 7.4), centrifuged at 200 *g* for 7 min, and suspended in 0.320 mmol/L sucrose buffered with HEPES (pH 7.4) and 0.1 mM EDTA-Na. The protein level was measured using the Bradford method, with human immunoglobulin as standard. The protein concentration in suspension was about 2 mg/ml in Ab melanoma cells. The cells were immediately counted using a Trypan Blue assay and the tricarboxylic acid cycle (TAC) enzymatic activities were measured. Before the assay, samples were diluted to the desired protein concentration in 0.2 % Triton X-100. PDHC activity was assayed by the citrate synthase coupled method followed by citrate quantisation using citrate lyase [57]. Aconitase and ICDH activity were examined by a direct measurement of NAD reduction [58,59]. The influence of **1a** and **1b** on enzyme activities is presented as the half maximal inhibitory concentration (IC_{50}).

2.11. Energetic and oxidoreduction potential of cells

The energetic state was assayed by determining the content of ATP and NAD in cell extracts prepared from freeze-dried cells using 0.4 M perchloric acid ($HClO_4$300 μl) and centrifuged (14,000 rpm; 10 min, 4 °C). Supernatants were neutralized to pH 6 with 3 M K_3PO_4 and after 15 min on ice centrifuged again. The concentration of nucleotides in supernatants was measured by high-performance liquid chromatography (HPLC) with UV-DAD detection as described earlier [60].

3. Statistical analyses

The statistical analyses were performed using the data analysis software system STATISTICA version 12 from StatSoft Inc. (2016). Data are expressed as arithmetical means ± SD (Standard Deviation) or SEM (Standard Error of the Mean). The results were analyzed by a non-parametric tests: Jonckheere test (to determine the significance of a trend in data), Mann-Whitney *U* test and Steel test (to compare the differences between the examined groups). $p < 0.05$ was considered statistically significant.

4. Results

4.1. Cell viability (XTT)

There was a statistically significant decreasing trend of melanoma cells viability with the increasing **1a** and **1b** concentration (Fig. 3A, $p < 0.001$). Nevertheless, it seemed that compounds **1a** and **1b** caused a slight viability increase of Ma cells at a dose up to 10 μM and 1 μM respectively, but then a cytotoxic effect against this melanotic form was dose-dependent (Fig. 3A). Similar observation in Ab melanoma cells referred only to compound **1b** at a dose up to 1 μM after 72 h (Fig. 3A). After 48 h incubation, the IC_{50} for **1a** and **1b** against Ab melanoma reached 14.3 μM and 15.4 μM respectively (Fig. 3B). After additional 24 h, these values decreased to 3.4 μM and 7.8 μM respectively (data not shown). At a tenfold higher dose, 150 μM, with melanotic Ma melanoma, only over 30 % and over 40 % of cells showed mitochondrial changes for **1a** and **1b**, respectively (Fig. 3A, B).

The IC_{50} dose of dacarbazine, a chemotherapeutic against melanoma, reached about 70 μM for the Ab melanoma line, only after prolonged incubation for 72 h – a much more higher dose than for both examined acridine compounds (Fig. 3B). Among melanotic Ma melanoma cells over 60 % were still alive at a dose 150 μM of dacarbazine (Fig. 3A), similar to the examined acridine compounds.

4.2. Cell cycle changes

After incubation with **1a** the content of cells in S/G2/M phases did not change significantly in comparison to control, for both melanoma types, and there were 37 % and 21 % of Ab and Ma melanoma cells in these phases, respectively (Fig. 4B). However, as the result of Ab melanoma cell incubation with **1b**, the number of cells in S/G2/M phases decreased to 28 % after 48 h and, after an additional 24 h, the number of cells in G0/G1 phases decreased significantly to 29 % (Fig. 4B).

These changes were accompanied by a statistically significant increased number of cells in the sub-G0 area, which comprised 36 % of all Ab cells after 72 h incubation with **1b** (Fig. 4B). Thus, under the influence of **1b,** Ab melanoma cells were broken into fragments with decreased DNA content (sub G0 area), and dying cells were found to originate from all cell cycle phases. Under the same conditions, **1b** did not cause significant cell cycle changes among Ma melanoma cells.

4.3. Changes to the plasma membrane structure of dying cells

1a does not induce significant changes in the plasma membrane structure, such as the externalization of phosphatidylserine (An+; annexin-positive cells) among Ab melanoma cells (Table 1, Fig. 4A). When affected by its methylated form **1b**, about 40 % of Ab cells were An+ after 48 h ($p < 0.05$). This 40 % figure was made up of 16 %, which were An+PI- (early apoptotic) cells, and 24 % which were An+PI+ (late apoptotic) cells. With prolonged incubation time to 72 h, the content of An+ cells increased to 45 % (Table 1, Fig. 4A). Under the same culture conditions, after 72 h, the number of An+ Ma melanoma cells slightly decreased to 16 % and 13 % for **1a** and **1b** respectively (Table 1, Fig. 4A). **1a** and **1b** did not increase the number of necrotic cells (An-PI+) among Ab cells, with necrotic cells being at a level of 4–5 %, but **1a** induced a slight increase in necrotic cells among Ma cells to about 16 % (Table 1). Changes in dying Ab melanoma cell morphology are documented in the Supplementary material (S2. Morphological changes of Ab melanoma cells).

4.4. Caspase activation

After 48 h 9% of Ab melanoma cells had activated caspases (C+), but this group of cells increased significantly with time only under the influence of **1a** (Table 1). Its methylated form **1b** did not increase the number of C+ cells, even after 72 h, although an increased number of cells without activated caspases but with a damaged plasma membrane (C-PI+, cells in the final stage of apoptosis) was noticed (Table 1). Among Ma cells, the examined compounds did not affect caspase activation (Table 1).

4.5. ROS activation

Both melanoma lines show similar numbers of cells with the ROS activity, about 40 %. These values did not change in Ma melanoma cells in the presence of either acridine compound, however in Ab melanoma cells it increased slightly to 61 % and 58 %, after 48 h incubation, with **1a** and **1b** respectively (Table 1, statistically insignificant).

It was observed that **1a** increased the content of cells with activated caspases among Ab melanoma cells, but with only slight PS

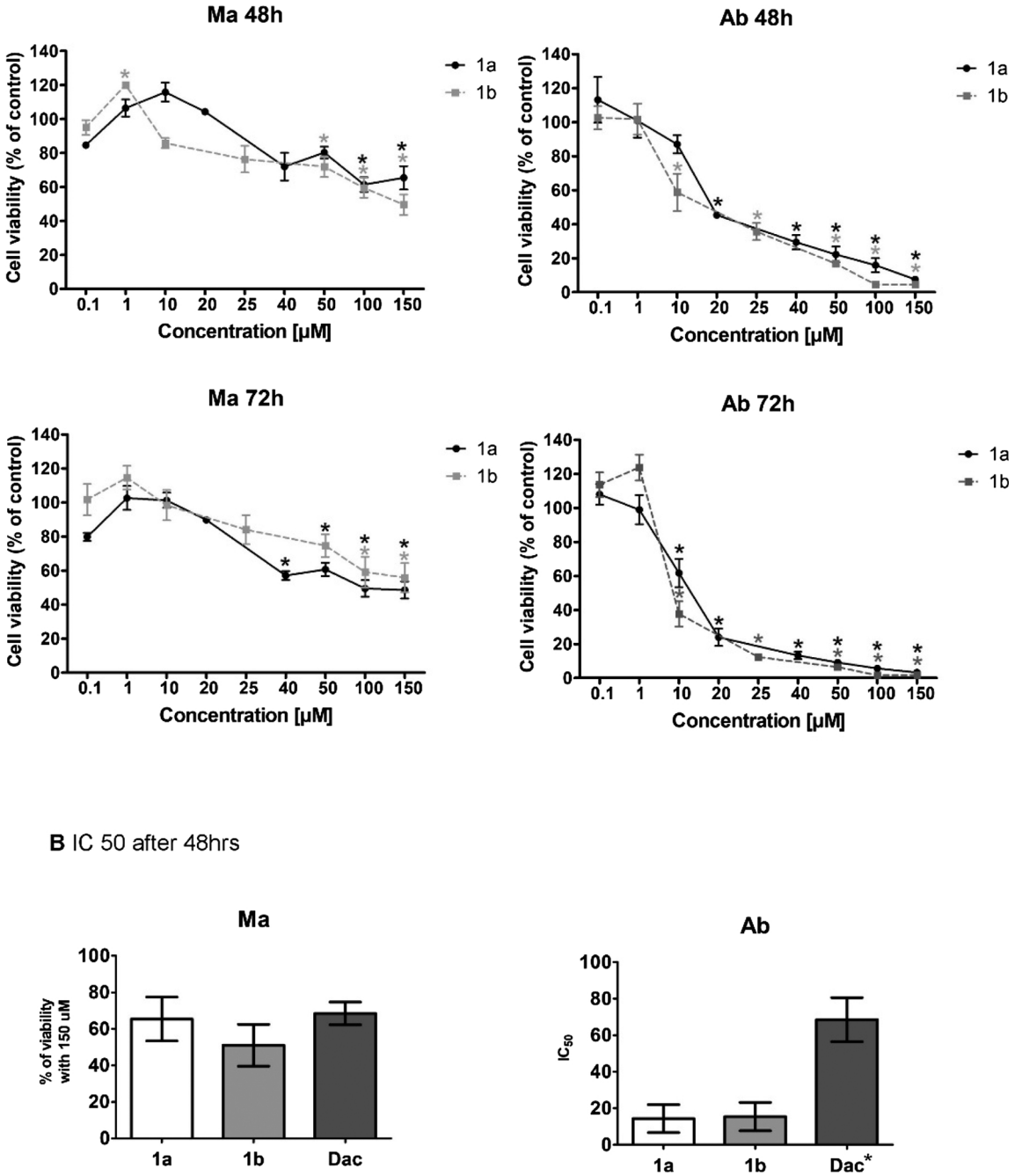

Fig. 3. Cytotoxicity of **1a**, **1b** and dacarbazine against Ma melanotic melanoma and Ab amelanotic melanoma. **A.** Cell XTT viability test. **B.** IC 50 dose of **1a**,**1b** and dacarbazine for Ab cells. Viability of Ma cells under 150 μM of **1a**,**1b** and dacarbazine. Dac* IC50 after 72 h incubation. For both melanoma lines at least three experiments were done and values are presented as mean ± SEM. Statistically significant change ($p < 0.05$) in comparison to control values. * (black stars for 1a) * (grey stars for 1b).

externalization (early apoptotic plasma membrane change, statistically insignificant increase) and did not change the number of cells localized in the sub-G0 area (e.g. apoptotic bodies). The methylated form **1b** did not influence caspase activation although this compound significantly increased the number of cells with apoptotic plasma membrane changes (PS externalization) and the number of cells in sub-G0. Counting cells in a hemocytometer confirmed that the total number of cells decreased by about 30 % after incubation with **1b** for 48 h (data not shown). Both compounds slightly increased the number of cells with ROS presence.

Thus **1a** and its methylated form **1b** act on amelanotic Ab melanoma (melanogenesis is inhibited) but in different ways. It seems that apoptosis and caspase-independent death are the main routes toward Ab melanoma cell death. Due to the importance of energetic metabolism in the mechanism of cell death, we followed some elements of the energetic state of Ab cells after **1a** and **1b** action as the next step of our experiment.

4.6. Activity of enzymes associated with the energetic state of cells

4.6.1. Pyruvate dehydrogenase complex (PDHC)

The activity of PDHC in Ab cells in control was about 2.01 ± 0.06 nmols/min/mg of protein. There was a statistically significant decreasing trend of PDHC activity in Ab melanoma with the increasing **1a** and **1b** concentration (Fig. 5A, $p < 0.05$ and $p < 0.001$ respectively).

A. Apoptotic plasma membrane changes - externalization of phosphatidylserine

Ma melanotic melanoma

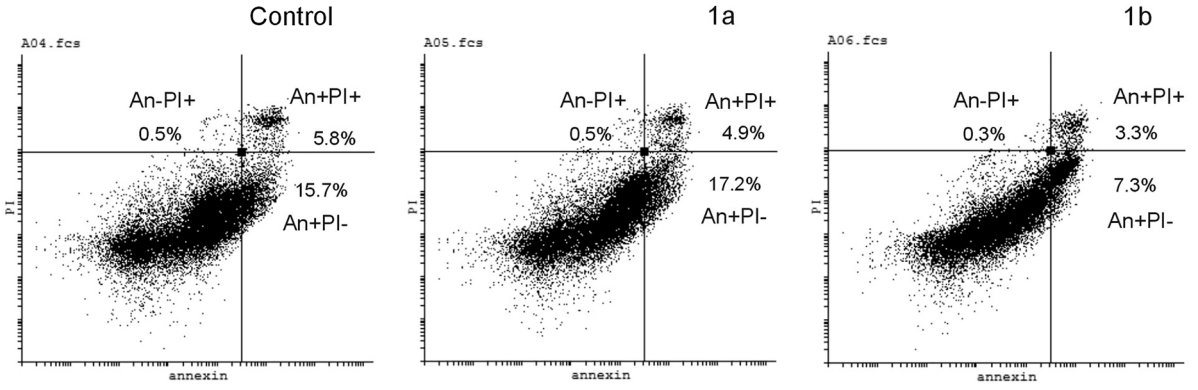

Ab amelanotic melanoma

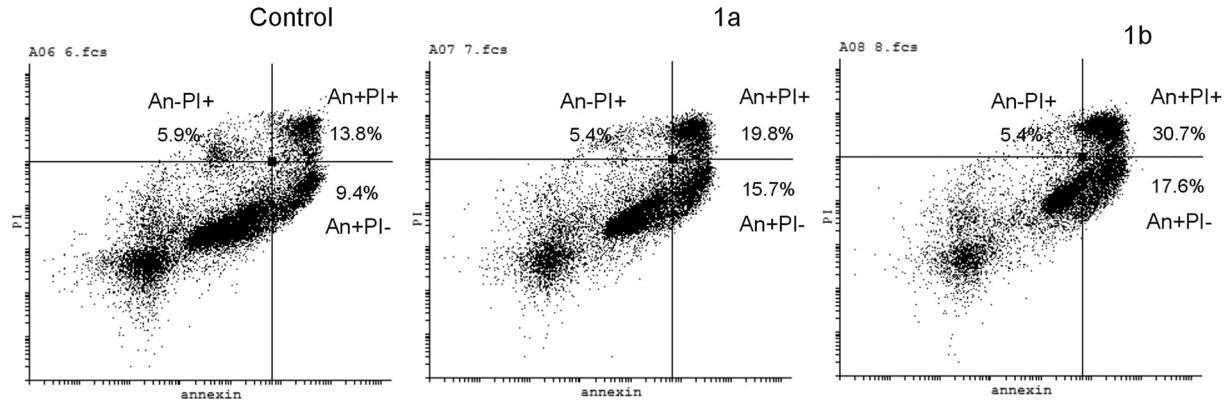

B. Cell cycle analysis

Cell line		Percentage of cells in cell cycle phases				Percentage of cells in Sub G0	
		G0/G1		S and G2/M			
Incubation time in hours		48	72	48	72	48	72
Ma melanoma	Control	56±12	53±9	24±4	19±3	16±8	24±12
	1a	58±3	55±3	21±4	19±5	18±6	24±8
	1b	53±12	50±3	20±2	18±2	25±14	30±4
Ab melanoma	Control	44±6	43±9	38±8	28±8	17±7	26±10
	1a	42±4	35±10	37±7	33±4	18±5	27±9
	1b	42±3	**29±9***	**28±7***	30±4	**28±7***	36±12

Fig. 4. Elements of the potential mechanism of **1a** and **1b** cytotoxicity. **A.** Flow cytometry analysis of one representative experiment that documents the apoptotic change in plasma membrane structure; PS externalization results analysis: An + PI- (early apoptotic), An + PI + (late apoptotic)), An-PI + (necrotic) after 48 h incubation without (control) and with **1a**,**1b**. **B.** The cell cycle analysis showing percentage of cells in cell cycle phases: G0/G1, S/G2/M, and cells with decreased DNA content (sub G0). Melanoma lines at least three experiments were done and values are presented as mean ± SD. * Statistically significant change ($p < 0.05$) in comparison to control values.

Table 1
The action of **1a** and **1b** on melanotic Ma and amelanotic Ab melanoma cells in terms of regulated cell death features, namely caspase activation (cells with activated caspases C+ and without active caspases but damaged plasma membrane C-PI+), phosphatidylserine externalization [cells with PS externalization An+, among them are early apoptotic An+PI- and late apoptotic An+PI+, and also cells without PS externalization but staining propidium iodide (PI) An-PI+] and ROS production. Melanoma lines at least three experiments were done and values are given as mean ± SD. * Statistically significant change ($p < 0.05$) in comparison to control values.

Percentage of cells with	Melanotic melanoma Ma						Amelanotic melanoma Ab					
	48 h			72 h			48 h			72 h		
	control	+1a	+1b	control	+ 1a	+1b	control	+ 1a	+1b	control	+ 1a	+1b
1. **Activated caspases**												
All C+	7.2 ± 6.6	4.2 ± 2.8	1.8 ± 0.8	5.5 ± 4.2	4.4 ± 3.9	2.9 ± 3.1	9.0 ± 4.2	**15.3 ± 5.0***	8.0 ± 1.0	16.3 ± 6.2	20.5 ± 7.9	9.6 ± 3.7
Final apoptotic/Necrotic C-PI+	4.4 ± 2.9	3.3 ± 2.2	6.4 ± 2.4	3.8 ± 1.6	3.2 ± 1.6	5.5 ± 2.6	4.1 ± 2.0	4.4 ± 0.6	**14.4 ± 4.7***	2.9 ± 1.6	3.5 ± 2.3	**13.5 ± 4.1***
2. Phosphatidylserine externalization												
All An+	24.7 ± 10	19.6 ± 6.9	9.4 ± 2.6	21.8 ± 8.0	16.3 ± 9.6	13.2 ± 10.9	24.5 ± 10.2	33.4 ± 11.4	**39.8 ± 9.7***	32.6 ± 10.8	35.6 ± 8.4	**45.1 ± 6.3***
Early apoptotic An+/PI-							10.6 ± 5.7	14.0 ± 5.9	15.6 ± 4.4	11.8 ± 7.2	15.4 ± 4.0	**25.2 ± 4.6***
Late apoptotic An+/PI+							13.9 ± 6.6	19.4 ± 5.7	**24.2 ± 6.5***	21.8 ± 7.5	20.2 ± 4.5	19.9 ± 2.6
Final apoptotic/Necrotic An-/PI+	4.0 ± 4.3	1.9 ± 1.4	5.1 ± 3.3	2.3 ± 1.7	**16.3 ± 9.6***	4.0 ± 2.7	5.3 ± 2.6	3.7 ± 1.7	3.6 ± 1.8	3.7 ± 2.3	5.9 ± 5.2	4.5 ± 4.0
3. Reactive oxygen species (ROS)	42.9 ± 8.2	41.0 ± 11.4	38.4 ± 17.9	35.9 ± 12.1	38.0 ± 13.8	40.1 ± 19.7	47.9 ± 23.6	61.1 ± 9.7	57.6 ± 8.9	42.8 ± 20.4	53.7 ± 15.5	48.8 ± 13.0

Compound **1a** at a dose of 10 μM caused unexpected increase of the PDHC activity (statistically insignificant) while a dose of 50 μM almost totally inhibited PDHC activity (Fig. 5A, $p < 0.001$). On the other hand the enzyme's activity was inhibited by **1b** at a concentration dependent manner, IC_{50} for **1b** was 60 μM (Fig. 5A).

4.6.2. Aconitase

The activity of aconitase in control conditions after 48 h was 9.07 ± 0.87 nmol/min/mg of protein. There was a statistically significant decreasing trend of aconitase activity in Ab melanoma with the increasing **1a** and **1b** concentration (Fig. 5B, $p < 0.001$). **1a** and **1b** strongly inhibited the activity of aconitase, with IC_{50} values of 20 μM and 26 μM for **1a** and **1b** respectively (Fig. 5B).

4.6.3. NADP-isocitrate dehydrogenase (ICDH)

The activity of ICDH in Ab cells after 48 h, under control conditions, was 26.01 ± 1.6 nmol/min/mg of protein. There was a statistically significant decreasing trend of ICDH activity in Ab melanoma with the increasing **1a** and **1b** concentration (Fig.5C, $p < 0.001$). Compound **1a** at 5 μM concentration caused 30 % fall of ICDH activity while further concentration increase up to 100 μM caused 50 % inhibition of ICDH activity (Fig. 5C). This enzyme was particularly sensitive to **1b** with the IC_{50} 14 μM, while the IC50 for **1a** was over 60 μM (Fig. 5C). There was a slight increase of ICDH activity under 5 μM of **1b** treatment but it was not statistically significant.

4.6.4. Lactate dehydrogenase (LDH)

The activity of LDH in Ab cells after 48 h, under control conditions, was 1.501 ± 0.02 μmol/min/mg of protein. There was a decreasing trend of LDH activity in Ab melanoma cells with the increasing **1a** concentration (Fig. 5D, $p < 0.05$).

There was a strong direct correlation between PDHC and ICDH activities and total Ab melanoma cell number, in cells treated with **1b** but not **1a** (Fig. 6 A,C). On the other hand there was a direct correlation between aconitase and the total cell number in cells treated with **1a** and **1b** (Fig. 6 B).

4.7. NAD and ATP

The NAD level was decreased by 20 % and 35 % after 48 h incubation with **1a** and **1b**, respectively (Fig. 7A), while the corresponding ATP levels were depleted by 14 % and 46 %, respectively (Fig. 7B). This illustrates that more significant changes in ATP and NAD content in Ab melanoma cells appeared under the influence of the methylated compound **1b**.

5. Discussion

Our results indicate that 9-chloro-1-nitroacridine (**1a**) and its methylated derivative 9-chloro-4-methyl-1-nitroacridine (**1b**) affect melanotic and amelanotic melanoma in different ways. In comparison to melanotic Ma melanoma, its amelanotic form – characterized by absence of melanin production, higher proliferation rate, and higher malignancy – was particularly sensitive to the action of these chloroacridines.

The observed increase in damaged cells (located in the sub-G0 area), and decreasing number of cells in the G0/G1 and S/G2/M phases, indicated that **1b** induced Ab melanoma cell death independently of the cell cycle phase. We did not observe cell cycle arrest in any phases among either type of melanoma, although acridines interacting with DNA have caused cell cycle arrest in many tumor lines [61–65]. **1b** cytotoxicity also confirmed decreasing number of cells counting with a hemocytometer. Thus, we looked at elements of cell death machinery that might be regulated by **1a** and **1b** action, e.g. plasma membrane structure changes that could induce other cells to phagocytize dying apoptotic cells (phosphatidylserine externalization as an "eat me"

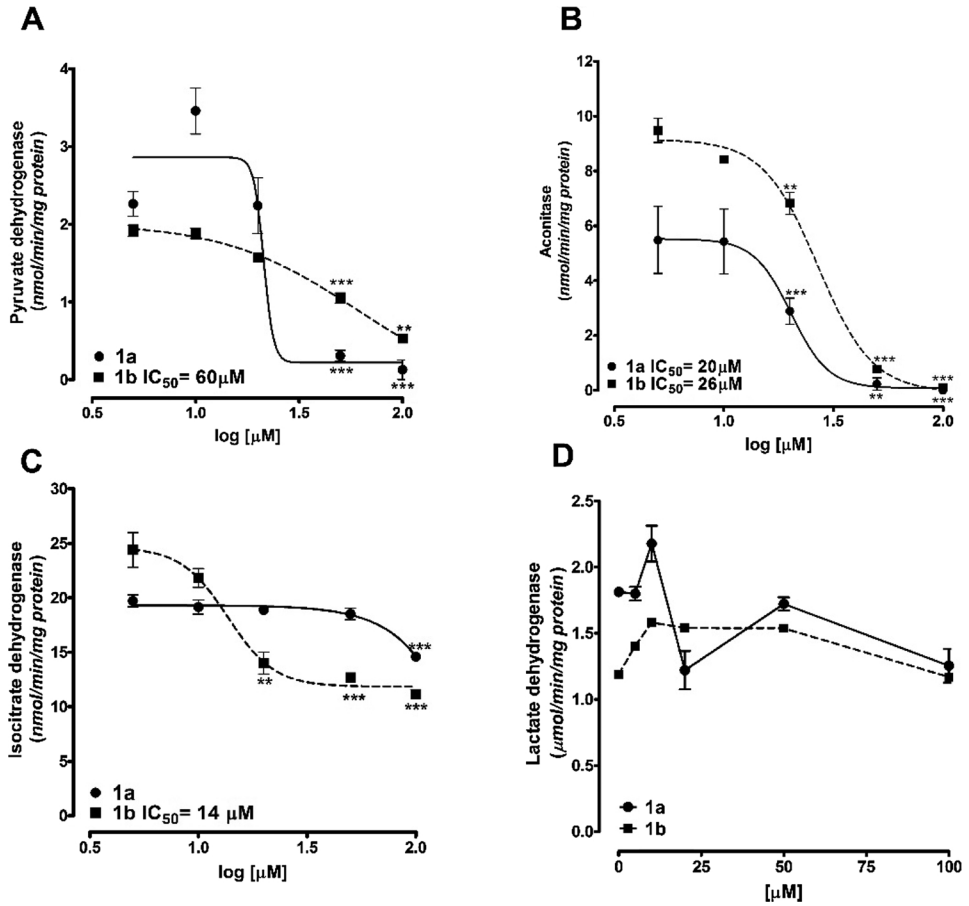

Fig. 5. Concentration-dependent effect of **1a** and **1b** incubated with Ab cells for 48 h on the activity of selected enzymes of the TCA cycle: **A**. PDHC, **B**. aconitase, **C**. ICDH, **D**. LDH. Data are given as mean ± SEM from 3-4 independent cellular cultures. Significantly different from respective control: *p < 0.05, ** p < 0.01,*** p < 0.001.

signal), caspase activation, energetic state (ATP, NAD), and activity of metabolic enzymes, in this case tricarboxylic acid cycle enzymes [66]. At a dose that inhibited 50 % of mitochondria, **1a** activated caspases with only slight PS externalization and without an increase in damaged cells localized in the sub-G0 phase (e.g. apoptotic bodies), while its methylated form **1b** did not influence caspase activation, yet significantly increased the level of cells with apoptotic plasma membrane changes (PS externalization), and those localized in the sub-G0 phase. Thus, **1b** seemed to destroy Ab melanoma cells more effectively than the unmethylated **1a,** but without involvement of caspases. Apoptosis which usually leads to caspase activation, is the best understood type of regulated cell death, but cells may also die by a process called caspase-independent cell death (CICD). Cells undergoing CICD produce several cytokines that are important for activation of the immune response [67–69]. It has been observed that this type of melanoma cell death does not stimulate cell proliferation, which is opposite to what is observed with the so-called apoptosis-induced proliferation [70]. Thus, it seems that cell death dependent and independent of caspase activation could be a mechanism by which these chloroacridine compounds act, although a detailed mechanism to explain the better effectiveness of **1b**

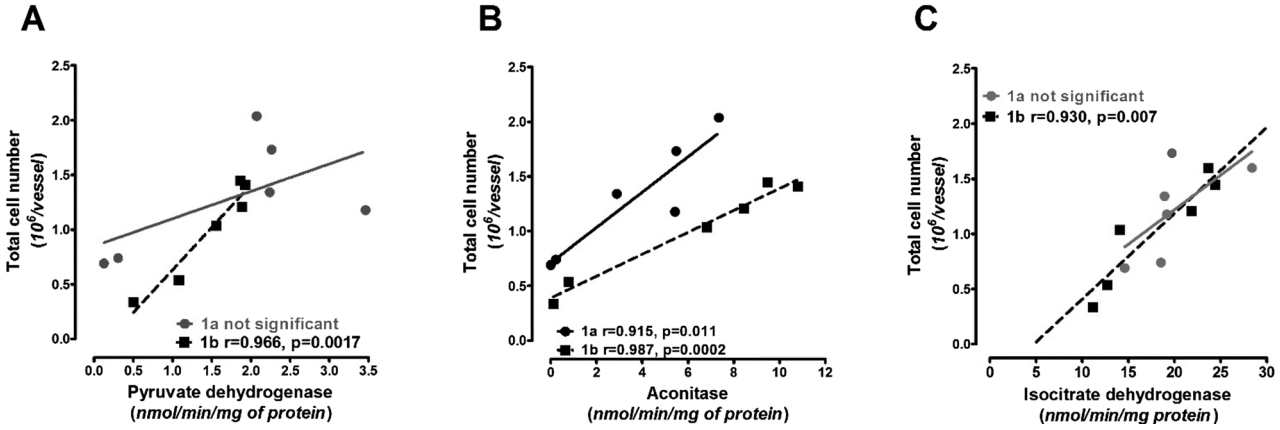

Fig. 6. The correlation between total cell number and PDHC (**A**), aconitase (**B**) and ICDH (**C**) activities in Ab cells after 48 h of incubation with **1b** or **1a.** Data are given as mean ± SEM from 3-6 independent cellular cultures.

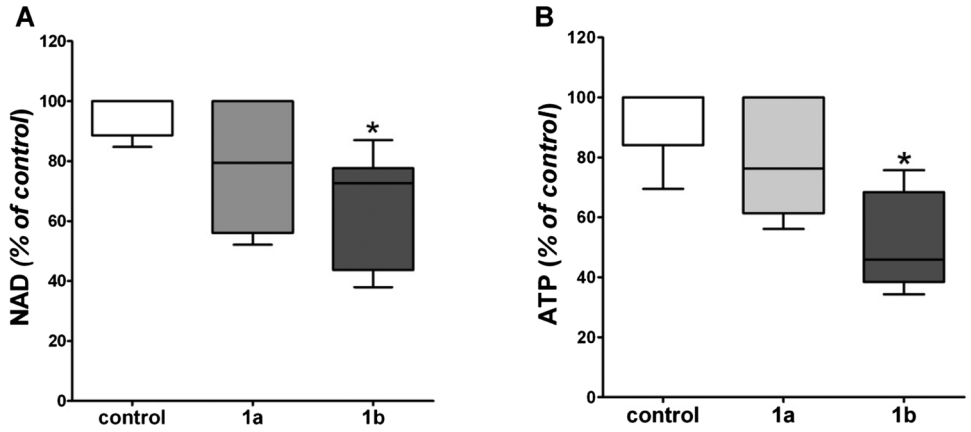

Fig. 7. The effect of 15 μM of **1a** and **1b** incubated with Ab cells for 48 h on levels of NAD (**A**) and ATP (**B**). Data are given as mean ± SEM from 3-6 independent cellular cultures. Significantly different from respective control:*$p < 0.05$.

against amelanotic melanoma needs further elucidation.

The energetic state analysis confirmed that cells dying as the result of the action of chloroacridines **1a** and **1b** lost ATP and NAD. Inhibition of examined metabolic enzymes, such as PDHC, aconitase and ICDH, was also observed. There is a lot of data showing that interference in the energy metabolism in cancer cells might be a successful therapeutic approach [71–74]. This is results from the fact that malignant cells favor conversion of glucose into lactate, instead of pyruvate, even when there is high oxygen pressure. This phenomenon was first described by Warburg, and is known as the Warburg effect [75]. However, activation of lactic acid fermentation does not supply ATP for all energy needs. In consequence, the Warburg metabolism is almost 100-fold faster than oxidative one, thanks to the high glucose influx [76]. Therefore, the mitochondria of cancer cells exhibit physiological disturbances that lead to malignancy development [77]. Moreover, there is data showing that changes in the micro-RNA of human melanocytes lead to disruption of normal cellular energy metabolism with anaerobic glycolysis [78]. Consequently, one of the mechanisms that could exert an anticancer effect could be interfering the activity of mitochondrial enzymes what could be the way of action. The strong correlation between ICDH activity with a total Ab melanoma cell number and stronger inhibition of ICDH activity as the result of **1b** action, indicated that compound **1b** interrupt the activity of carboxylic acid cycle enzymes. In tumor cells, the cytosolic form of the enzyme ICDH1 was found to support mitochondrial oxidative metabolism and NADPH synthesis by its mitochondrial isoenzyme ICDH2 [79]. This mechanism plays a role in decreasing mitochondrial ROS formation in cancer cells [79]. Therefore compounds that are able to inhibit the activity of ICDH activity can be considered to be a novel anticancer compound. **1b**, inhibiting ICDH activity more effectively than **1a**, was such a compound.

Additionally aconitase inhibition by **1b** could be a promising observation, as Gonzales-Sanchez et al. have noted that inhibition of this enzyme inhibits tumor growth, including in melanoma cells [80].

The significant ATP decrease in **1b**-treated cells was probably due to the decrease in total NAD level, initiated by the depletion of PDHC activity (NAD is a cofactor of the E2 subunit of PDHC). On the other hand, a slight increase of LDH activity observed with low concentration of **1a** may be the result of glycolytic pathway activation, as PDHC activity also increased in these conditions.

There are studies showing that, apart from oxygen from ATP production, mitochondrial respiration is needed to complement NAD [81]. Thus inhibition of aconitase activity can enhance NAD depletion.

The better effectiveness of **1b**, i.e. the methylated form of **1a**, against amelanotic melanoma, needs further examination. However, there are reports indicating that methylation of acridine (AMSA) improved its binding to DNA and DNA cleavage [82].

6. Conclusions

Our results indicated that melanotic and amelanotic melanomas responded to chloroacridine action in different ways. Elements of the regulated cell death pathways were observed only in amelanotic melanoma cells, although the methylated form of chloroacridine induced death without caspase activation (caspase-independent cell death); this needs further studying. The mechanism of the interrelationships between energy metabolism and cell death is not fully understood, though the fact that **1b** interferes with the activities of tricarboxylic acid cycle enzymes could be a way towards possible therapeutic use, especially against the amelanotic form of melanoma. As such it justified further studies.

Funding

This work was financially supported by the Polish National Science Center, grant no. 2014/13/B/NZ7/02234.

Authors' contribution

MC and AR analyzed and interpreted the data. MC performed tests for means of cell death, AR performed tests for enzyme activities, MD performed the viability test and IPN estimated ATP and ADP levels, MGK and KD performed acridine syntheses; MC, AR, and KD were the major contributors in writing the manuscript. All authors read and approved the final manuscript.

Ethical approval

All procedures performed in these studies which involved animals were in accordance with the ethical standards of the institution or practice at which the studies were conducted.

Declaration of Competing Interest

The authors declare that there are no conflict of interest.

Acknowledgement

We would like to thank professor Ewa Augustin from the Department of Pharmaceutical Technology and Biochemistry, Chemical Faculty, Gdansk University of Technology (Poland) for the flow cytometry analysis support.

Appendix A. Supplementary data

Supplementary material related to this article can be found, in the online version, at doi:https://doi.org/10.1016/j.biopha.2020.110515.

References

[1] S.A. Rosenberg, J.C. Yang, R.M. Sherry, U.S. Kammula, M.S. Hughes, G.Q. Phan, et al., Durable complete responses in heavily pretreated patients with metastatic melanoma using T cell transfer immunotherapy, Clin. Cancer Res. 17 (2011) 4550–4557, https://doi.org/10.1158/1078-0432.CCR-11-0116.

[2] A. Ribas, R. Kefford, M.A. Marshall, C.J. Punt, J.B. Haanen, M. Marmol, et al., Phase III randomized clinical trial comparing tremelimumab with standard-of care chemotherapy in patients with advanced melanoma, J. Clin. Oncol. 31 (2013) 616–622, https://doi.org/10.1200/JCO.2012.44.6112.

[3] J. Schachter, A. Ribas, G.V. Long, A. Arance, J.J. Grob, L. Mortier, et al., Pembrolizumab versus ipilimumab for advanced melanoma: final overall survival results of a multicentre, randomised, open-label phase 3 study (KEYNOTE-006), Lancet 390 (2017) 1853–1862, https://doi.org/10.1016/S0140-6736(17)31601–X.

[4] J.L. da Silva, A.L.S. Dos Santos, N.C.C. Nunes, F. de Moraes Lino da Silva, C.G.M. Ferreira, A.C. de Melo, Cancer immunotherapy: the art of targeting the tumor immune microenvironment, Cancer Chemother. Pharmacol. 84 (2019) 227–240, https://doi.org/10.1007/s00280-019-03894-3.

[5] M. Polkowska, P. Ekk-Cierniakowski, E. Czepielewska, W. Wysoczański, W. Matusewicz, M.J. Kozłowska-Wojciechowska MJ, Survival of melanoma patients treated with novel drugs: retrospective analysis of real-world data, Cancer Res. Clin. Oncol. Open Access 143 (2017) 2087–2094, https://doi.org/10.1007/s00432-017-2453-z.

[6] T. Swe, K.B. Kim, Update on systemic therapy for advanced cutaneous melanoma and recent development of novel drugs, Clin. Exp. Metastasis 35 (2018) 503–520 https://doi.org/0.1007/s10585-018-9913-y.

[7] P.R. Pereira, A.N. Odashiro, L.A. Lim, C. Miyamoto, P.L. BlancoL, M. Odashiro, et al., Current and emerging treatment options for uveal melanoma, Clin. Ophthalmol. 7 (2013) 1669–1682, https://doi.org/10.2147/OPTH.S28863.

[8] S. Mourah, B. Louveau, N. Dumaz, Mechanisms of resistance and predictive biomarkers of response to targeted therapies and immunotherapies in metastatic melanoma, Curr. Opin. Oncol. 32 (2020) 91–97, https://doi.org/10.1097/CCO.0000000000000603.

[9] M. Cichorek, M. Wachulska, A. Stasiewicz, A. Tymińska, Skin melanocytes: biology and development, Postepy Dermatol. Alergol. 30 (2013) 30–41, https://doi.org/10.5114/pdia.2013.33376.

[10] R. Rabbie, P. Ferguson, C. Molina-Aguilar, D.J. Adams, C.D. Robles-Espinoza, Melanoma subtypes: genomic profiles, prognostic molecular markers and therapeutic possibilities, J. Pathol. 247 (2019) 539–551, https://doi.org/10.1002/path.5213.

[11] G. Palmieri, M.N. Ombra, M. Colombino, M. Casula, M.C. Sini, A. Manca, et al., Multiple molecular pathways in melanomagenesis: characterization of therapeutic targets, Front. Oncol. 5 (2015) 183, https://doi.org/10.3389/fonc.2015.00183.

[12] H.A. Mejbel, S.K.C. Arudra, D. Pradhan, C.A. Torres-Cabala, P. Nagarajan, M.T. Tetzlaff, et al., Immunohistochemical and molecular features of melanomas exhibiting intratumor and intertumor histomorphologic heterogeneity, Cancers (Basel) 11 (2019) 1714, https://doi.org/10.3390/cancers11111714.

[13] F. Rambow, J.-Ch. Marine, C.R. Goding, Melanoma plasticity and phenotypic diversity: therapeutic barriers and opportunities, Genes Dev. (33) (2019) 1295–1318, https://doi.org/10.1101/gad.329771.119.

[14] T. Grzywa, W. Paskal, P. Wlodarski, Intratumor and intertumor heterogeneity in melanoma, Transl. Oncol. 10 (2017) 956–975, https://doi.org/10.1016/j.tranon.2017.09.007.

[15] L. Boeckmann, A.C. Nickel, C. Kuschal, A. Schaefer, K.M. Thoms, M.P. Schön, et al., Temozolomide chemoresistance heterogeneity in melanoma with different treatment regimens: DNA damage accumulation contribution, Melanoma Res. 21 (2011) 206–216, https://doi.org/10.1097/CMR.0b013e328345af95.

[16] S.C. Searles, E.K. Santosa, J.D. Bui, Cell-cell fusion as a mechanism of DNA exchange in cancer, Oncotarget 9 (2017) 6156–6173, https://doi.org/10.18632/oncotarget.23715.

[17] A. Avagliano, G. Fiume, A. Pelagalli, G. Sanità, M.R. Ruocco, S. Montagnani, A. Arcucci, Metabolic plasticity of melanoma cells and their crosstalk with tumor microenvironment, Front. Oncol. 10 (2020) 722, https://doi.org/10.3389/fonc.2020.00722.

[18] R. Avolio, D.S. Matassa, D. Criscuolo, M. Landriscina, F. Esposito, Modulation of mitochondrial metabolic reprogramming and oxidative stress to overcome chemoresistance in cancer, Biomolecules 10 (2020) 135, https://doi.org/10.3390/biom10010135.

[19] M. Saez-Ayala, M.F. Montenegro, L. Sanchez-Del-Campo, M.P. Fernandez-Perez, S. Chazarra, R. Freter, et al., Directed phenotype switching as an effective antimelanoma strategy, Cancer Cell 24 (2013) 105–119, https://doi.org/10.1016/j.ccr.2013.05.009.

[20] F.G. Cordaro, A.L. De Presbiteris, R. Camerlingo, N. Mozzillo, G. Pirozzi, E. Cavalcanti, et al., Phenotype characterization of human melanoma cells resistant to dabrafenib, Oncol. Rep. 38 (2017) 2741–2751, https://doi.org/10.3892/or.2017.5963.

[21] F. Ahmed, N.K. Haass, Microenvironment-driven dynamic heterogeneity and phenotypic plasticity as a mechanism of melanoma therapy resistance, Front. Oncol. (2018) 173, https://doi.org/10.3389/fonc.2018.00173.

[22] R. Fisher, L. Pusztai, C. Swanton, Cancer heterogeneity: implications for targeted therapeutics, Br. J. Cancer 108 (2013) 479–485, https://doi.org/10.1038/bjc.2012.581.

[23] J. Tsoi, L. Robert, K. Paraiso, C. Galvan, K.M. Sheu, J. Lay, et al., Multi-stage differentiation defines melanoma subtypes with differential vulnerability to drug-induced iron-dependent oxidative stress, Cancer Cell 33 (2018) 890–904, https://doi.org/10.1016/j.ccell.2018.03.017 e5.

[24] E. Wee, R. Wolfe, C. Mclean, J.W. Kelly, Y. Pan, Clinically amelanotic or hypomelanotic melanoma: anatomic distribution, risk factors, and survival, J. Am. Acad. Dermatol. 79 (2018) 645–651, https://doi.org/10.1016/j.jaad.2018.04.045.

[25] A. Slominski, T.K. Kim, A. Brozyna, Z. Janjetovic, D.L.P. Brooks, L.P. Schwab, et al., The role of melanogenesis in regulation of melanoma behavior: melanogenesis leads to stimulation of HIF-1α expression and HIF-dependent attendant pathways, Arch. Biochem. Biophys. 56 (3) (2014) 79–93, https://doi.org/10.1016/j.abb.2014.06.030.

[26] H.Z. Gong, H.Y. Zheng, J. Li, Amelanotic melanoma, Melanoma Res. 29 (2019) 221–230, https://doi.org/10.1097/CMR.0000000000000571.

[27] L. Gualandri, R. Betti, C. Crosti, Clinical features of 36 cases of amelanotic melanomas and considerations about the relationship between histologic subtypes and diagnostic delay, J. Eur. Acad. Dermatol. Venereol. 23 (2009) 283–287, https://doi.org/10.1111/j.1468-3083.2008.03041.

[28] N.E. Thomas, A. Kricker, W.T. Waxweiler, P.M. Dillon, K.J. Busman, L. From L, et al., Comparison of clinicopathologic features and survival of histopathologically amelanotic and pigmented melanomas: a population-based study, JAMA Dermatol. 150 (2014) 1306–1314, https://doi.org/10.1001/jamadermatol.2014.1348.

[29] T. Wasiewicz, P. Szyszka, M. Cichorek, Z. Janjetovic, R.C. Tuckey, A.T. Slominski, et al., Antitumor effects of vitamin D analogs on hamster and mouse melanoma cell lines in relation to melanin pigmentation, Int. J. Mol. Sci. 16 (2015) 6645–6667, https://doi.org/10.3390/ijms16046645.

[30] K.G. Chen, R.D. Leapman, G. Zhang, B. Lai, J.C. Valencia, C.O. Cardarelli, et al., Influence of melanosome dynamics on melanoma drug sensitivity, J. Natl. Cancer Inst. 101 (2009) 1259–1271, https://doi.org/10.1093/jnci/djp259.

[31] B.S. Larsson, Interaction between chemicals and melanin, Pigment Cell Res. 6 (1993) 127–133, https://doi.org/10.1111/j.1600-0749.1993.tb00591.x.

[32] M. Pawlikowska, J. Piotrowski, T. Jędrzejewski, W. Kozak, A.T. Slominski, A.A. Brożyna, Coriolus versicolor-derived protein-bound polysaccharides trigger the caspase-independent cell death pathway in amelanotic but not melanotic melanoma cells, Phytother. Res. 34 (2020) 173–183, https://doi.org/10.1002/ptr.6513.

[33] M. Gensicka-Kowalewska, G. Cholewiński, K. Dzierzbicka, Recent developments in the synthesis and biological activity of acridine/acridone analogues, RSC Adv. 7 (2017) 15776–15804, https://doi.org/10.1039/C7RA01026E.

[34] M. Kukowska M, Amino acid or peptide conjugates of acridine/acridone and quinoline/quinolone-containing drugs. A critical examination of their clinical effectiveness within a twenty-year timeframe in antitumor chemotherapy and treatment of infectious diseases, Eur. J. Pharm. Sci. 109 (2017) 587–615, https://doi.org/10.1016/j.ejps.2017.08.027.

[35] K. Pawlak, J.W. Pawlak, J. Konopa, Cytotoxic and antitumor activity of 1-nitroacridines as an after effect of their interstrand DNA cross-linking, Cancer Res. 44 (1984) 4289–4296.

[36] G. Moloney, D. Kelly, P. Mack, Synthesis of acridine-based DNA bis-intercalating agents, Molecules 6 (2001) 230–243, https://doi.org/10.3390/2F60300230.

[37] Z. Mazerska, J. Dziegielewski, J. Konopa, Enzymatic activation of a new antitumour drug, 5-diethylaminoethylamino-8-hydroxyimidazoacridinone, C-1311, observed after its intercalation into DNA, Biochem. Pharmacol. 61 (2001) 685–694, https://doi.org/10.1016/s0006-2952(01)00527-5.

[38] B. Zhang, X. Li, B. Li, C. Gao, Y. Jiang, Acridine and its derivatives: a patent review (2009 – 2013), Expert Opin. Ther. Patents 24 (2014) 647–664, https://doi.org/10.1517/13543776.2014.902052.

[39] J. Jesek, J. Hlavacek, J. Sebestik, Biomedical applications of acridines, in: K.D. Rainsford (Ed.), Progress in Drug Research 72, Springer International Publishing AG, 2017, pp. 1–243, , https://doi.org/10.1007/978-3-319-63953-6_5.

[40] M. Cichorek, A. Ronowska, M. Gensicka-Kowalewska, M. Deptula, I. Pelikant-Malecka, K. Dzierzbicka, Novel therapeutic compound acridine-retrotuftsin action on biological forms of melanoma and neuroblastoma, J. Cancer Res. Clin. Oncol. 145 (2019) 165–179, https://doi.org/10.1007/s00432-018-2776-4.

[41] M. Gensicka-Kowalewska, K. Dzierzbicka, M. Cichorek, M. Deptuła, A. Ronowska, Synthesis new analogs of 4-methyl-1-nitroacridine and its biological evaluation as potential anticancer drugs, Asian J. Pharmaceut, Anal. Med. Chem. 6 (2018) 42–60.

[42] R.M. Acheson, Acridines, Interscience Publishers, NY, London, 1973.

[43] A. Achari, S. Neidle, 9-Chloroacridine, Acta Cryst B33 (1977) 3269–3270.

[44] G. Rouband, R. Faure, J.P. Galy, H-1 and C-13 chemical shifts for acridines: part XVIII. 9-chloroacridine and 9-(N-allyl)- and 9-(N-propargyl)acridinamine derivatives, Magn. Reson. Chem. 41 (2003) 549–553, https://doi.org/10.1002/mrc.1170.

[45] A. Ledochowskl, Ledacrin - anticancerous medicine 1-nitro-9(3-dimethyloamino-propylamino)-acridine-2HCl-H2O, Mater. Med. Pol. 8 (1976) 237–251.

[46] K. Dzierzbicka, A.M. Kołodziejczyk, B. Wysocka-Skrzela, A. Myśliwski, D. Sosnowska, Synthesis and antitumor activity of conjugates of muramyldipeptide, normuramyl dipeptide, and desmuramylpeptides with acridine/acridone derivatives, J. Med. Chem. 44 (2001) 3606–3615, https://doi.org/10.1021/jm001115g.

[47] K. Dzierzbicka, A.M. Kołodziejczyk, Synthesis and antitumor activity of conjugates of muramyldipeptide or normuramyldipeptide with hydroxy-acridine/acridone derivatives, J. Med. Chem. 46 (2003) 183–189, https://doi.org/10.1021/jm001115g.

[48] M. Robin, R. Faure, A. Perichaud, J.P. Galy, Synthesis of new thiazolo[5,4-a]acridine derivatives, Heterocycles 53 (2000) 387–395, https://doi.org/10.3987/COM-

99-8794.
[49] B.T. Ashok, K. Tadi, D. Banerjee, J. Konopa, M. Iatropoulos, R.K. Tiwari, Pre-clinical toxicology and pathology of 9-(2′-hydroxyethylamino)-4-methyl-1-nitroacridine (C-1748), a novel anti-cancer agent in male Beagle dogs, Life Sci. 79 (2006) 1334–1342, https://doi.org/10.1016/j.lfs.2006.03.043.
[50] A. Bomirski, A. Slomiński, J. Bigda, The natural history of a family of transplantable melanomas in hamsters, Cancer Metastasis Rev. 7 (1988) 95–118, https://doi.org/10.1007/bf00046481.
[51] M. Sniegocka, E. Podgórska, P.M. Płonka, M. Elas, B. Romanowska-Dixon, M. Szczygieł, et al., Transplantable melanomas in hamsters and gerbils as models for human melanoma. Sensitization in melanoma radiotherapy-from animal models to clinical trials, Int. J. Mol. Sci. 19 (2018) 1048, https://doi.org/10.3390/ijms19041048.
[52] K. Zielińska, K. Kozłowska, M. Cichorek, M. Wachulska, Fas and FasL expression on cells of two transplantable melanoma lines according to their different biological properties, Folia Histochem. Cytobiol. 46 (2008) 337–343, https://doi.org/10.2478/v10042-008-0041-4.
[53] M. Gensicka-Kowalewska, M. Cichorek, A. Ronowska, M. Deptula, I. Klejbor, K. Dzierzbicka, Synthesis and biological evaluation of acridine/acridone analogs as potential anticancer agents, Med. Chem. (Los Angeles) 15 (2019) 729–737, https://doi.org/10.2174/1573406414666181015145120.
[54] J.K. Konopa, B. Wysocka-Skrzela, R. Tiwari, 9-Alkylamino-1-nitroacridine derivatives. WO 2001/60801A2, patent published 2001-08-23. (2001).
[55] P. Smolewski, J. Grabarek, H. Halicka, Z. Darżynkiewicz, Assay of caspase activation in situ combined with probing plasma membrane integrity to detect three distinct stages of apoptosis, J. Immunol. Methods 265 (2002) 111–121, https://doi.org/10.1016/s0022-1759(02)00074-1.
[56] M. Cichorek, Camptothecin-induced death of amelanotic and melanotic melanoma cells in different phases of cell cycle, Neoplasma 58 (2011) 227–234, https://doi.org/10.4149/neo_2011_03_227.
[57] A. Szutowicz, M. Stepien, G. Piec, Determination of pyruvate dehydrogenase and acetyl-CoA synthetase activities using citrate synthase, Anal. Biochem. 115 (1981) 81–88, https://doi.org/10.1016/0003-2697(81)90527-3.
[58] J. Villafranca, The mechanism of aconitase action: evidence for an enzyme isomerization by studies of inhibition by tricarboxylic acids, J. Biol. Chem. 249 (1974) 6149–6155.
[59] G.W. Plaut, T. Aogaichi, Purification and properties of diphosphopyridine nucleotide-linked isocitrate dehydrogenase of mammalian liver, J. Biol. Chem. 243 (1968) 5572–5583.
[60] R. Smolenski, D. Lachno, S. Ledingham, M. Yacoub, Determination of sixteen nucleotides, nucleosides and bases using high-performance liquid chromatography and its application to the study of purine metabolism in hearts for transplantation, J. Chromatogr. 527 (1990) 414–420, https://doi.org/10.1016/s0378-4347(00)82125-8.
[61] T.L. Su, T.C. Chou, J.Y. Kim, J.T. Huang, G. Ciszewska, W.Y. Ren, et al., 9-substituted acridine derivatives with long half-life and potent antitumor activity: synthesis and structure-activity relationships, J. Med. Chem. 38 (1995) 3226–3235, https://doi.org/10.1021/jm00017a006.
[62] I. Antonini, DNA-binding antitumor agents: from pyrimido 5,6,1-de/acridines to other intriguing classes of acridine derivatives, Curr. Med. Chem. 9 (2002) 1701–1716, https://doi.org/10.2174/092986702336926.
[63] J. Polewska, A. Skwarska, E. Augustin, J. Konopa, DNA-damaging imidazoacridinone C-1311 induces autophagy followed by irreversible growth arrest and senescence in human lung cancer cells, J. Pharmacol. Exp. Ther. 346 (2013) 393–405, https://doi.org/10.1124/jpet.113.203851.
[64] A. Skladanowski, Modulation of G(2) arrest enhances cell death induced by the antitumor 1-nitroacridine derivative, Nitracrine, Apoptosis 7 (2002) 347–359, https://doi.org/10.1023/a:1016127513947.
[65] S. Almeida, A. Ribeiro, G. de Lima Silva, J. Ferreira Alves, E. Beltrao, et al., DNA binding and Topoisomerase inhibition: How can these mechanisms be explored to design more specific anticancer agents? Biomed. Pharmacother. 96 (2017) 1538–1556, https://doi.org/10.1016/j.biopha.2017.11.054.
[66] L. Galluzzi, I. Vitale, S.A. Aaronson, J.M. Abrams, D. Adam, P. Agostinis, et al., Molecular mechanisms of cell death: recommendations of the Nomenclature Committee on Cell Death 2018, Cell Death Differ. 25 (2018) 486–541, https://doi.org/10.1038/s41418-017-0012-4.
[67] N. Yatim, H. Jusforgues-Saklani, S. Orozco, O. Schulz, R. Barreira da Silva, C. Reis e Sousa, et al., RIPK1 and NF-κB signaling in dying cells determines cross-priming of $CD8^+$ T cells, Science 350 (2015) 328–334, https://doi.org/10.1126/science.aad0395.
[68] E. Giampazolias, B. Zunino, S. Dhayade, F. Bock, C. Cloix, K. Cao, et al., Mitochondrial permeabilization engages NF-κB-dependent anti-tumour activity under caspase deficiency, Nat. Cell Biol. 19 (2017) 1116–1129, https://doi.org/10.1038/ncb3596.
[69] E. Giampazolias, S.W.G. Tait, Caspase-independent cell death: an anti-cancer double whammy, Cell Cycle 17 (2018) 269–270, https://doi.org/10.1080/15384101.2017.1408229.
[70] A. Roumane, K. Berthenet, C. El Fassi, G. Ichim, Caspase-independent cell death does not elicit a proliferative response in melanoma cancer cells, BMC Cell Biol. 19 (2018) 11, https://doi.org/10.1186/s12860-018-0164-1.
[71] L. Xu, L. Wang, L. Zhou, R.G. Dorfman, Y. Pan, D. Tang, et al., The SIRT2/cMYC pathway inhibits peroxidation-related apoptosis in cholangiocarcinoma through metabolic reprogramming, Neoplasia 29 (2019) 429–441, https://doi.org/10.1016/j.neo.2019.03.002.
[72] E. Andreucci, S. Pietrobono, S. Peppicelli, J. Ruzzolini, F. Bianchini, A. Biagioni, et al., SOX2 as a novel contributor of oxidative metabolism in melanoma cells, Cell Commun. Signal 16 (2018) 87, https://doi.org/10.1186/s12964-018-0297-z.
[73] G. Pathria, D.A. Scott, Y. Feng, J. Sang Lee, Y. Fujita, G. Zhang, et al., Targeting the Warburg effect via LDHA inhibition engages ATF4 signaling for cancer cell survival, EMBO J. 37 (20) (2018), https://doi.org/10.15252/embj.201899735 pii: e99735.
[74] T.A. Fedele, A.C. Galdos-Riveros, H. Jose de Farias e Melo, A. Magalhaes, D.A. Maria, Prognostic relationship of metabolic profile obtained of melanoma B16F10, Biomed. Pharmacother. 67 (2013) 146–156, https://doi.org/10.1016/j.biopha.2012.10.013.
[75] O. Warburg, On respiratory impairment in cancer cells, Science 124 (1956) 269–270.
[76] A. Maus, G.J. Peters, Glutamate and α-ketoglutarate: key players in glioma metabolism, Amino Acids 49 (2017) 21–32, https://doi.org/10.1007/s00726-016-2342-9.
[77] S. Vyas, E. Zaganjor, M.C. Haigis, Mitochondria and cancer, Cell 28 (2016) 555–566, https://doi.org/10.1016/j.cell.2016.07.002.
[78] H. Kaushik, D. Malik, D. Parsad, D. Kaul, Mitochondrial respiration is restricted by miR-2909 within human melanocytes, Pigment Cell Melanoma Res. 32 (2018) 584–587, https://doi.org/10.1111/pcmr.12758.
[79] L. Jiang, A.A. Shestov, P. Swain, C. Yang, S.J. Parker, Q.A. Wang, et al., Reductive carboxylation supports redox homeostasis during anchorage-independent growth, Nature 532 (2016) 255–258, https://doi.org/10.1038/nature17393.
[80] L. Gonzalez-Sanchez, M.A. Cobos-Fernandez, P. Lopez-Nieva, M. Villa-Morales, K. Stamatakis, J.M. Cuezva, et al., Exploiting the passenger ACO1-deficiency arising from 9p21 deletions to kill T-cell lymphoblastic neoplasia cells, Carcinogenesis (2019), https://doi.org/10.1093/carcin/bgz185 pii: bgz185.
[81] K. Birsoy, T. Wang, W.W. Chen, E. Freinkman, M. Abu-Remaileh, D.M. Sabatini, An essential role of the mitochondrial electron transport chain in cell proliferation is to enable aspartate synthesis, Cell 162 (2015) 540–551, https://doi.org/10.1016/j.cell.2015.07.016.
[82] A.C. Ketron, W.A. Denny, D.E. Graves, N. Osheroff, Amsacrine as a topoisomerase II poison: importance of Drug-DNA interactions, Biochemistry 51 (2012) 1730–1739, https://doi.org/10.1021/bi201159b.